Res Chem Intermed
DOI 10.1007/s11164-013-1440-5

Synthesis, structure, antioxidation, and DNA-binding studies of a binuclear ytterbium(III) complex with bis(*N*-salicylidene)-3-oxapentane-1,5-diamine

Huilu Wu · Guolong Pan · Yuchen Bai · Hua Wang · Jin Kong · Furong Shi · Yanhui Zhang · Xiaoli Wang

Received: 10 June 2013 / Accepted: 8 October 2013

Abstract A new complex of ytterbium(III) nitrate with bis(*N*-salicylidene)-3-oxapentane-1,5-diamine (H_2L), with the composition $Yb_2(L)_2(NO_3)_2{\cdot}2H_2O$, was synthesized and characterized by physic-chemical and spectroscopic methods. The crystal structure of the ytterbium(III) complex has been determined by single-crystal X-ray diffraction. It reveals a centrosymmetric binuclear neutral entity where Yb(III) metal centers are bridged by two phenoxo oxygen atoms. Electronic absorption titration spectra, ethidium bromide displacement experiments, and viscosity measurements indicate that both the ligand and the Yb(III) complex can bind calf thymus DNA, presumably via a groove binding mechanism. Furthermore, the antioxidant activities of the Yb(III) complex were determined by a superoxide and hydroxyl radical scavenging method in vitro, which indicates that it is a scavenger for OH and O_2^- radicals.

Keywords Bis(*N*-salicylidene)-3-oxapentane-1,5-diamine · Ytterbium(III) complex · Crystal structure · DNA-binding property · Antioxidant activity

Introduction

It is well known that deoxyribonucleic acid (DNA) is an important genetic substance in organism. The regions of DNA involved vital processes, such as gene expression, gene transcription, mutagenesis, and carcinogenesis [1, 2]. Numerous biological experiments have demonstrated that DNA is the primary intracellular

H. Wu (✉) · G. Pan · Y. Bai · H. Wang · J. Kong · F. Shi · Y. Zhang · X. Wang
School of Chemical and Biological Engineering, Lanzhou Jiaotong University, Lanzhou 730070, People's Republic of China
e-mail: wuhuilu@163.com

Published online: 25 October 2013

target of anticancer drugs. Interaction between small molecules and DNA can cause damage in cancer cells, blocking the division, and resulting in cell death [3, 4]. The biological activities shown by DNA binder metal complexes are various and are often related to their specific DNA-binding mechanism, ranging from intercalation to covalent and groove binding [5, 6]. Therefore, research on the mechanism of the interaction of complexes with DNA is attracting more and more attention. The results will potentially be useful in the design of new compounds that can recognize specific sites or conformations of DNA [7–9].

Lanthanide metal complexes have been used as biological models to understand the structures of biomolecules and biological processes [10]. One of the most studied applications is the use of lanthanide complexes to address DNA/RNA by non-covalent binding and/or cleavage [11, 12]. In addition, Schiff bases are able to inhibit the growth of several animal tumors, and some metal chelates have shown good antitumor activities against animal tumors [13]. So, well-designed organic ligands enable a fine tuning of special properties of the metal ions. In this study, a Schiff base ligand and its ytterbium(III) complex were synthesized and characterized. Their DNA-binding behavior and antioxidant ability were investigated.

Experimental

Materials and methods

All chemicals were of analytical grade. Calf thymus DNA (CT-DNA), EB, nitroblue tetrazolium nitrate (NBT), methionine (MET), and riboflavin ($VitB_2$) were obtained from Sigma-Aldrich (USA) and used without purification. The stock solution of ligand and complex were dissolved in DMF at the concentration 3×10^{-3} M. All experiments involving interaction of the ligand and the complex with CT-DNA were carried out in double-distilled water buffer containing 5 mM Tris and 50 mM NaCl adjusted to pH 7.2 with hydrochloric acid. A solution of CT-DNA gave a ratio of UV absorbance at 260 and 280 nm of about 1.8–1.9, indicating that the CT-DNA was sufficiently free of protein [34]. The CT-DNA concentration per nucleotide was determined spectrophotometrically by employing an extinction coefficient of 6,600 M^{-1} cm^{-1} at 260 nm [35].

C, H, and N elemental analyses were determined using a Carlo Erba 1106 elemental analyzer. IR spectra were recorded from 4,000 to 400 cm^{-1} with a Nicolet FT-VERTEX 70 spectrometer using KBr pellets. Electronic spectra were taken on Lab-Tech UV Bluestar and Spectrumlab 722sp spectrophotometers and the spectral resolution used was 0.2 nm. Fluorescence spectra were recorded on a LS-45 spectrofluorophotometer. ^1H NMR spectra were obtained with a Mercury plus 400 MHz NMR spectrometer with TMS as internal standard and $CDCl_3$ as solvent.

The synthetic route for the ligand precursor H_2L is shown in Scheme 1.

3-Oxapentane-1,5-diamine

3-Oxapentane-1,5-diamine was synthesized following the procedure in Ref. [36]. Calcd. (%) for $C_4H_{12}N_2O$: C, 46.25; H, 11.54; N, 26.90. Found (%): C, 45.98; H,

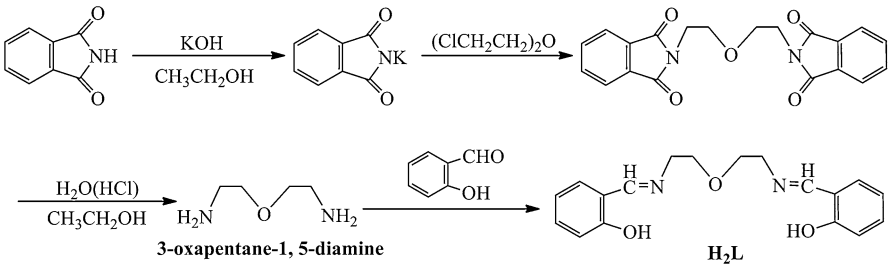

Scheme 1 Schematic diagram showing the synthesis of ligand H_2L

11.50; N, 26.76. FT–IR (KBr ν/cm^{-1}): 1,120, ν(C–O-C); 3,340, ν(–NH_2) stretching frequency, respectively.

Bis(N-salicylidene)-3-oxapentane-1,5-diamine (H_2L)

For the synthesis of H_2L, salicylic aldehyde (10 mmol, 1.22 g) in EtOH(5 mL) was added dropwise into a 5-mL EtOH solution of 3-oxapentane-1,5-diamine (5 mmol, 0.52 g). Then, the solution was stirred for 4 h at 78 °C. After cooling to room temperature, the precipitate was filtered. The product was dried in vacuo, and a yellow crystalline solid obtained. Yield: 1.19 g (68.5 %). Calcd. (%) for $C_{18}H_{20}O_3N_2$: C, 69.21; H, 6.45; N, 8.97. Found (%): C, 69.09; H, 6.54; N, 8.83. ^{1}H NMR ($CDCl_3$ 400 MHz) δ/ppm: 8.30 (s, 2H, N=C–H), 6.79–7.33 (m, 8H, H-benzene ring), 3.66–3.74 (m, 8H, O-$(CH_2)_2$-N=C). UV–Vis (λ, nm): 268, 316. FT–IR (KBr ν/cm^{-1}): 1,637, ν(C=N); 1,286, ν(C–O–C); 3,458, ν(OH) stretching frequency, respectively.

$Yb_2L_2(NO_3)_2{\cdot}2H_2O$

To a stirred solution of H_2L (0.156 g, 0.5 mmol) in EtOH (10 mL) was added $Yb(NO_3)_3(H_2O)_6$ (0.234 g 0.5 mmol) and triethylamine (0.3 mL) in EtOH (10 mL). The yellow sediment generated rapidly. The precipitate was filtered off, washed with EtOH and absolute Et_2O, and dried in vacuo. The dried precipitate was dissolved in DMF to form a yellow solution. The yellow block crystals of the Yb(III) complex suitable for X-ray diffraction studies were obtained by vapor diffusion of diethyl ether into the solution for few weeks at room temperature. Yield: 0.204 g (54.7 %). Calcd. (%) for $C_{36}H_{40}N_6O_{14}Yb$: C, 38.19; H, 3.55; N, 7.45. Found (%): C, 38.19; H, 3.73; N, 7.21. UV–Vis (λ, nm): 269, 317. FT–IR (KBr ν/cm^{-1}): 1,244, ν(C–O–C); 1,388, 1,057, ν(NO_3); 1,633, ν(C=N) stretching frequency, respectively.

X-ray crystallography

A suitable single crystal was mounted on a glass fiber, and the intensity data were collected on a Bruker Smart CCD diffractometer with graphite-monochromated Mo

-Kα radiation (λ = 0.71073 Å) at 296 K. Data reduction and cell refinement were performed using the SMART and SAINT programs [37]. The structure was solved by direct methods and refined by full-matrix least-squares against F^2 of data using SHELXTL software [38]. All H atoms were found in difference electron maps and subsequently refined in a riding-model approximation with C–H distances ranging from 0.93 to 0.97 Å and U_{iso} (H) = 1.2 or 1.5 U_{eq}(C). The crystal data and experimental parameters relevant to the structure determination are listed in Table 1. Selected bond lengths and angles are presented in Table 2.

Crystallographic data (excluding structure factors) for the structure in this paper have been deposited with the Cambridge Crystallographic Data Centre, CCDC, 12 Union Road, Cambridge CB2 1EZ, UK. Copies of the data can be obtained free of charge on quoting the depository number CCDC-929560 (Fax: +44-1223-336-033; e-mail: deposit@ccdc.cam.ac.uk, http://www.ccdc.cam.ac.uk).

Table 1 Crystal and structure refinement data for $Yb_2L_2(NO_3)_2{\cdot}2H_2O$

Complex	$Yb_2L_2(NO_3)_2{\cdot}2H_2O$
Molecular formula	$C_{36}H_{40}N_6O_{14}Yb_2$
Molecular weight	1,126.82
Color, habit	Yellow, block
Crystal size, mm^3	0.26 × 0.24 × 0.22
Crystal system	Monoclinic
Space group	*C2/c*
a, Å	29.108(7)
b, Å	11.666(3)
c, Å	15.195(4)
β, °	118.842(2)
V, $Å^3$	4,519.7(19)
Z	4
Absorption coefficient, mm^{-1}	4.178
T, K	296(2)
D_{calcd}, g cm^{-3}	1.656
F (000), e	2,200
θ range for data collection, °	2.20−25.50
hkl range	±35, ±14, ±18
Reflections collected	14,161
Independent reflections/R_{int}	4,184/0.0346
Data/restraints/parameters	4,184/3/262
Final R_1/wR_2 indices [$I > 2\sigma(I)$]	0.0285/0.0713
R_1/wR_2 indices (all data)[a]	0.0433/0.0776
Goodness-of-fit on F^2	1.108
Largest diff. peak/hole, e $Å^{-3}$	0.955/−0.797

Table 2 Selected bond lengths (Å) and bond angles (°) for $Yb_2L_2(NO_3)_2{\cdot}2H_2O$

Bond lengths			
Yb(1)−O(3)	2.134(4)	Yb(1)−O(1)	2.428(4)
Yb(1)−O(2)#1[a]	2.247(3)	Yb(1)−N(2)	2.442(5)
Yb(1)−O(2)	2.277(3)	Yb(1)−O(4)	2.460(4)
Yb(1)−O(5)	2.424(4)	Yb(1)−N(1)	2.463(5)
Bond angles			
O(3)−Yb(1)−O(2)#1	96.77(14)	O(3)−Yb(1)−O(2)	84.37(13)
O(2)#1−Yb(1)−O(2)	71.05(14)	O(3)−Yb(1)−O(5)	95.60(16)
O(2)#1−Yb(1)−O(5)	156.71(13)	O(2)−Yb(1)−O(5)	129.94(14)
O(3)−Yb(1)−O(1)	141.44(14)	O(2)#1−Yb(1)−O(1)	87.29(12)
O(2)−Yb(1)−O(1)	132.36(13)	O(5)−Yb(1)−O(1)	70.86(14)
O(3)−Yb(1)−N(2)	75.23(17)	O(2)#1−Yb(1)−N(2)	85.17(14)
O(2)−Yb(1)−N(2)	146.56(15)	O(5)−Yb(1)−N(2)	79.00(15)
O(1)−Yb(1)−N(2)	66.90(17)	O(3)−Yb(1)−O(4)	81.31(15)
O(2)#1−Yb(1)−O(4)	149.88(12)	O(2)−Yb(1)−O(4)	78.86(12)
O(5)−Yb(1)−O(4)	51.98(13)	O(1)−Yb(1)−O(4)	112.97(13)
N(2)−Yb(1)−O(4)	122.62(14)	O(3)−Yb(1)−N(1)	150.67(15)
O(2)#1−Yb(1)−N(1)	90.54(14)	O(2)−Yb(1)−N(1)	71.20(14)
O(5)−Yb(1)−N(1)	88.27(16)	O(1)−Yb(1)−N(1)	67.01(15)
N(2)−Yb(1)−N(1)	133.86(17)	O(4)−Yb(1)−N(1)	78.31(15)

[a] Symmetry transformations used to generate equivalent atoms: #1 $-x + 1/2, -y + 1/2, -z$

DNA-binding experiments

Viscosity experiments were conducted on an Ubbelohde viscometer, immersed in a water bath maintained at 25.0 ± 0.1 °C. The flow time was measured with a digital stopwatch and each sample was tested three times to get an average calculated time. Titrations were performed for the complexes (3–30 μM), and each compound was introduced into the CT-DNA solution (42.5 μM) present in the viscometer. Data were analyzed as $(\eta/\eta_0)^{1/3}$ versus the ratio of the concentration of the compound to CT-DNA, where η is the viscosity of CT-DNA in the presence of the compound and η_0 is the viscosity of CT-DNA alone. Viscosity values were calculated from the observed flow time of CT-DNA-containing solutions corrected from the flow time of buffer alone (t_0), $\eta = (t - t_0)$ [7].

Absorption titration experiments were performed with fixed concentrations of the complexes, while gradually increasing the concentration of CT-DNA. To obtain the absorption spectra, the required amount of CT-DNA was added to both the compound and reference solutions, in order to eliminate the absorbance of CT-DNA itself. From the absorption titration data, the binding constant (K_b) was determined using the equation [39]:

$$[\mathrm{DNA}]/(\varepsilon_a - \varepsilon_f) = [\mathrm{DNA}]/(\varepsilon_b - \varepsilon_f) + 1/K_b(\varepsilon_b - \varepsilon_f),$$

where [DNA] is the concentration of CT-DNA in base pairs, ε_a corresponds to the observed extinction coefficient (Aobsd/[M]), ε_f corresponds to the extinction

coefficient of the free compound, ε_b is the extinction coefficient of the compound when fully bound to CT-DNA, and K_b is the intrinsic binding constant. The ratio of slope to intercept in the plot of [DNA]/($\varepsilon_a - \varepsilon_f$) versus [DNA] gave the value of K_b.

The enhanced fluorescence of EB in the presence of DNA can be quenched by the addition of a second molecule [40]. The extent of fluorescence quenching of EB bound to CT-DNA can be used to determine the extent of binding between the second molecule and CT-DNA. Competitive binding experiments were carried out in the buffer by keeping [DNA]/[EB] = 1 and varying the concentrations of the compounds. The fluorescence spectra of EB were measured using an excitation wavelength of 520 nm, and the emission range was set between 550 and 750 nm. The spectra were analyzed according to the classical Stern–Volmer equation [9]:

$$I_0/I = 1 + K_{SV}[Q],$$

where I_0 and I are the fluorescence intensities at 599 nm in the absence and presence of the quencher, respectively, K_{SV} is the linear Stern–Volmer quenching constant, and [Q] is the concentration of the quencher. In these experiments, [CT-DNA] = 2.5×10^{-3} mol/L and [EB] = 2.2×10^{-3} mol/L.

Antioxidant study methods

Hydroxyl radicals were generated in aqueous media through the Fenton-type reaction [41]. The aliquots of reaction mixture (3 mL) contained 1 mL of 0.1 mmol aqueous safranin, 1 mL of 1.0 mmol aqueous EDTA–Fe(II), 1 mL of 3 % aqueous H_2O_2, and a series of quantitative microadditions of solutions of the test compound. A sample without the tested compound was used as the control. The reaction mixtures were incubated at 37 °C for 30 min in a water bath. The absorbance was then measured at 520 nm. All the tests were run in triplicate and are expressed as the mean and standard deviation (SD) [42]. The scavenging effect for OH· was calculated from the following expression:

$$\text{Scavenging ratio } (\%) = [\,(A_i - A_0)\,/\,(A_c - A_0)\,] \times 100\ \%,$$

where A_i is the absorbance in the presence of the test compound, A_0 is the absorbance of the blank, A_c is the absorbance in the absence of the test compound, EDTA-Fe(II), and H_2O_2.

A nonenzymatic system containing 1 mL 9.9×10^{-6} M $VitB_2$, 1 mL 1.38×10^{-4} M NBT, and 1 mL 0.03 M MET was used to produce superoxide anion (O_2^-), and the scavenging rate of O_2^- under the influence of 0.1–1.0 μM of the tested compound was determined by monitoring the reduction in rate of transformation of NBT to monoformazan dye [43]. The solutions of MET, $VitB_2$, and NBT were prepared with 0.02 M phosphate buffer (pH 7.8) in the condition of avoiding light. The reactions were monitored at 560 nm with a UV–Vis spectrophotometer, and the rate of absorption change was determined. The percentage inhibition of NBT reduction was calculated using the following equation [44]: percentage inhibition of NBT reduction = $(1 - k'/k) \times 100$, where k' and k present the slopes of the straight line of absorbance values as a function of time in the presence and absence of superoxide dismutase mimic compound, respectively. The IC_{50} values for the complexes were determined by plotting the graph

of percentage inhibition of NBT reduction against the increase in the concentration of the complex. The concentration of the complex which causes 50 % inhibition of NBT reduction is reported as IC_{50}.

Results and discussion

The Yb(III) complex, $Yb_2(L)_2(NO_3)_2{\cdot}2H_2O$, was prepared by reaction of H_2L with $Yb(NO_3)_3(H_2O)_6$ in ethanol. It is soluble in polar aprotic solvents such as DMF, DMSO, and MeCN, slightly soluble in ethanol, methanol, ethyl acetate, and chloroform, and insoluble in water, Et_2O, and petroleum ether. Elemental analysis shows that its composition is $Yb_2(L)_2(NO_3)_2{\cdot}2H_2O$ which was confirmed by the crystal structure analysis.

X-ray structure of the complex

The prepared pentadentate ligand contains strong donors, namely phenoxo oxygen atoms as well as imine nitrogen atoms, with an excellent coordination ability for transition/inner-transition metal ions through its N_2O_3 donor set. The crystal structure of the Yb(III) complex consists of discrete $Yb_2(L)_2(NO_3)_2$ and two water-solvent molecules. Single-crystal X-ray structure determination has revealed that the complex has a centrosymmetric neutral homobinuclear entity. An ORTEP illustration of the complex (Fig. 1) shows that two adjacent [Yb(L)(NO_3)] moieties are bridged via two phenoxo groups. In the μ_2-diphenoxo-bridged binuclear structure, both Yb(III) centers are octa-coordinated (Fig. 2a). The local coordination environment is identical for both the centers by symmetry, and is best described as a distorted square YbN_2O_6 antiprism (Fig. 2b). Due to the flexibility of the ligand, it loses its planarity. The bond lengths are in the range Yb(1)–N_{imine} 2.442(5)–2.463(5), Yb(1)–O_{ether} 2.428(4), and Yb(1)–$O_{nitrate}$ 2.424(4)–2.460(4) Å. The nature of coordination of the two Schiff base moieties of the same ligand is completely different. Of the two phenoxo oxygen atoms of each ligand, one is simply mono-coordinated while the other one bridges the adjacent Yb(III) centers, as reflected by the Yb–$O_{phenoxo}$ bond lengths [Yb(1)–O(2) 2.277(3) and Yb(1)–O(3) 2.134(4) Å]. The distance Yb(1)–Yb(1A) of 3.6824(10) Å is too long to consider any direct intramolecular Yb–Yb bonding.

An interesting feature of this structure is the intermolecular hydrogen bond that exists among the Yb(III) complexes, which also leads to large solvent-accessible voids which might trap guest molecules (Fig. 3). Thus, the solid may have the potential for practical applications such as gas absorption [14]. It is worth noting that intermolecular interactions have the potential to assemble smaller and simpler fragments into desired cavities under favorable conditions, which is important in host–guest chemistry and has applications in chemistry, biology, and materials science.

IR and electronic spectra

For the free ligand H_2L, a strong band is found at 1,637 cm^{-1} together with a weak band at 1,286 cm^{-1}. By analogy with previous assignments, the former can be

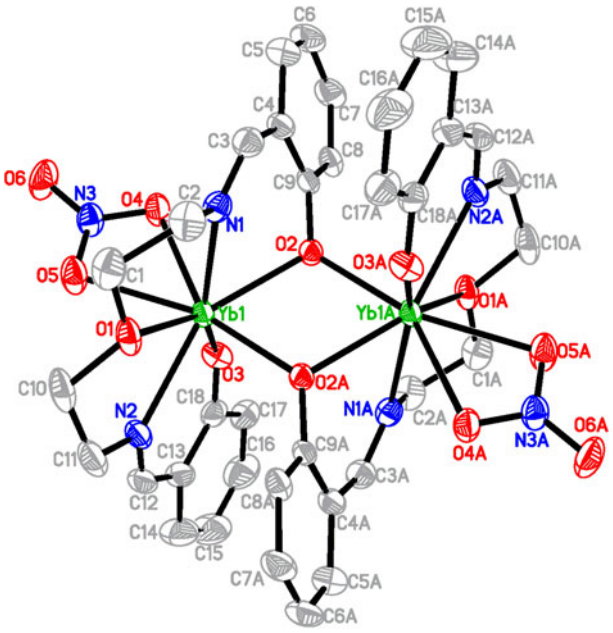

Fig. 1 The molecular structure of the Yb(III) complex in the crystal with displacement ellipsoids at the 30 % probability level; H atoms are omitted for clarity

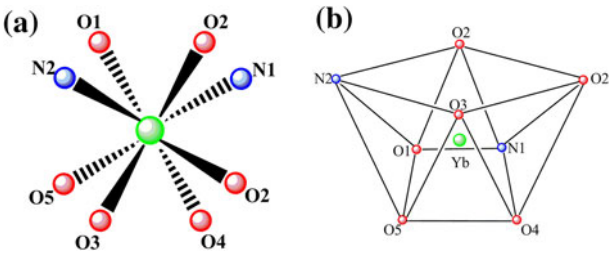

Fig. 2 **a** Perspective disposition of the donor sites around each Yb^{3+} center shown in Neumann projection. **b** A distorted square antiprism geometry is formed by donor atoms around the Yb^{3+} center as illustrated in the polyhedral view

attributed to *v*(C=N), while the latter can be attributed to *v*(C–O–C). These bands were shifted to lower frequencies by ca. 4–42 cm^{-1} for the Yb(III) complex [15], which implies direct coordination of the nitrogen and oxygen atoms to the metal ion. Bands at 1,388 and 1,057 cm^{-1} indicate that nitrate is bidentate [16], in agreement with the result of X-ray diffraction.

The electronic spectra of the ligand H_2L and the Yb(III) complex were recorded in DMF solution at room temperature. The UV bands of H_2L (268 and 316 nm) are marginally shifted in the complex. The two absorption bands are assigned to $\pi \rightarrow \pi^*$ (benzene) and $\pi \rightarrow \pi^*$ (C=N) transitions [17].

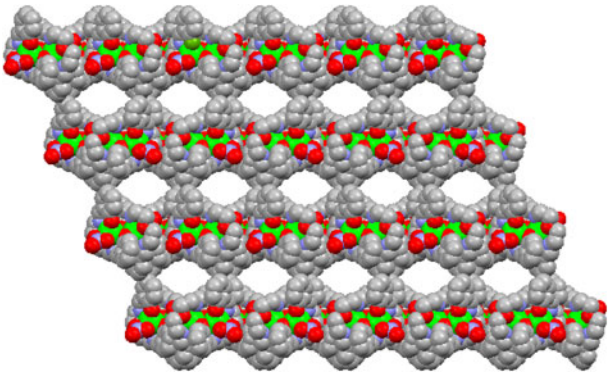

Fig. 3 A space-filling diagram of the nanosized holes in Yb(III) complex (in order to simplify, water-solvent molecules are omitted for clarity)

DNA binding properties

In order to clarify the interaction nature between the investigated compounds and DNA, viscosity measurement was carried out. Hydrodynamic measurements that are sensitive to changes in the length of DNA (i.e. viscosity and sedimentation) are regarded as the least ambiguous and the most critical tests of binding in solution in the absence of crystallographic structural data [18]. The classic intercalation model involves the insertion of a planar molecule between DNA base pairs, which results in a decrease in the DNA helical twist and lengthening of the DNA; the molecule will also be in close proximity to the DNA base pairs [19]. In contrast, a partial and/or non-classical intercalation of the complex in the DNA grooves typically causes low (positive or negative) or no change in DNA solution viscosity [20].

The effects of the ligand and of the Yb(III) complex on the viscosity of CT-DNA are shown in Fig. 4. The experimental results show that the addition of H_2L and complex causes no significant viscosity change. Therefore, according to the previously reported relationship to DNA-binding lanthanide complexes [5, 20, 21], we can deduce that the ligand and the Yb(III) complex most probably bind to DNA in a groove mode.

The application of electronic absorption spectroscopy in DNA-binding studies is one of the most useful techniques [8]. To clarify the interactions between the compounds and DNA, the electronic absorption spectra of the ligand and the Yb(III) complex in the absence and presence of the CT-DNA (at a constant concentration of the compounds) were obtained, which are shown in Fig. 5. With increasing DNA concentrations, the absorption bands at 394 nm of H_2L show a hypochromism of 32.35 %; the absorption bands at 393 nm of the Yb(III) complex show a hypochromism of 60.82 %. The hypochromism observed for the $\pi \rightarrow \pi^*$ transition bands indicating strong binding of H_2L and complex to DNA.

To quantitatively compare the affinity of H_2L and the Yb(III) complex towards DNA, the intrinsic binding constants K_b of the two compounds to CT-DNA were determined by monitoring the changes of absorbance with increasing concentration

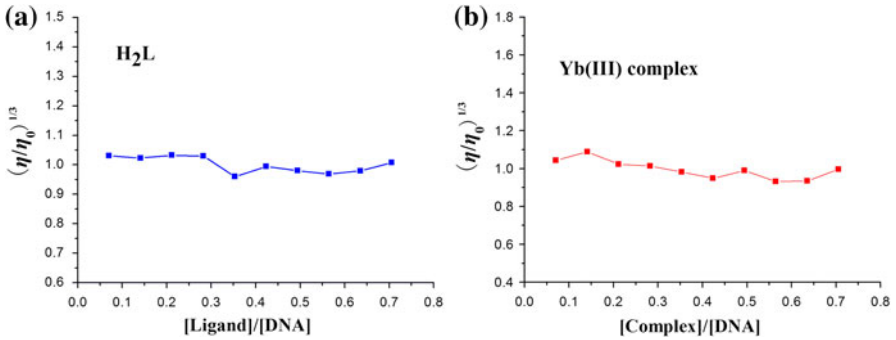

Fig. 4 Effect of increasing amounts of **a** H_2L and **b** Yb(III) complex on the relative viscosity of CT-DNA at 25.0 ± 0.1 °C

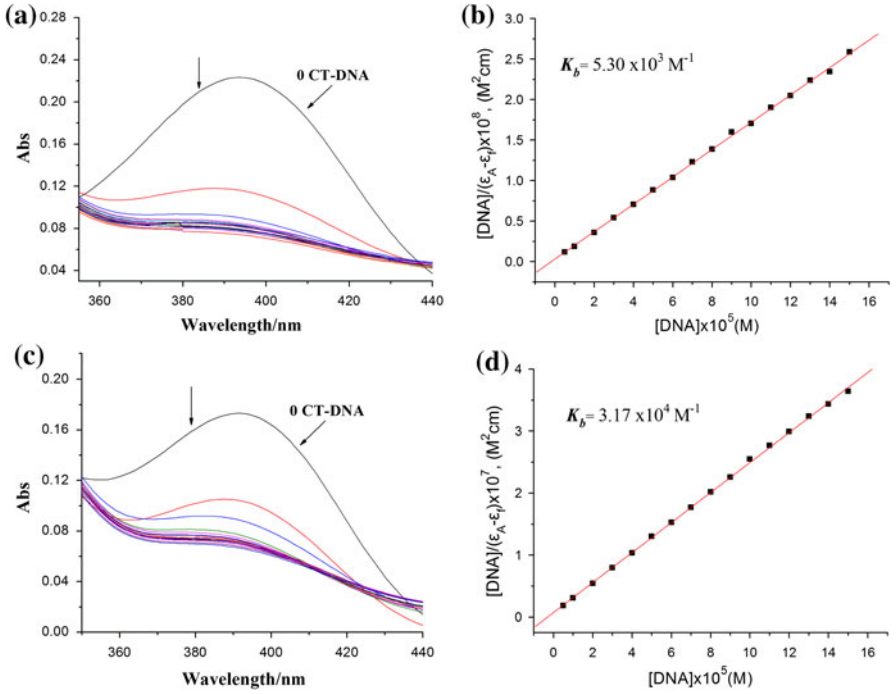

Fig. 5 Electronic spectra of **a** H_2L, **c** Yb(III) complex in Tris–HCl buffer upon addition of CT-DNA. [Compound] = 3.0×10^{-5} M, [DNA] = 2.5×10^{-5} M. *Arrow* shows the absorbance intensity changes upon increasing DNA concentration. Plots of [DNA]/($\varepsilon_a - \varepsilon_f$) vs. [DNA] for the titration of **b** H_2L, **d** Yb(III) complex with CT-DNA

of DNA. The intrinsic binding constant K_b of H_2L and of the Yb(III) complex were 5.30×10^3 M^{-1} ($R = 0.99$ for 16 points) and 3.17×10^4 M^{-1} ($R = 0.99$ for 16 points), respectively, from the decay of the absorbances. The results indicate that the binding strength of the complex is higher than for H_2L. Moreover, the K_b value

obtained here is lower than that reported for classical intercalator {for EB and $[Ru(phen)DPPZ]^{2+}$ and some Ln complexes whose binding constants have been found to be in the order of 10^6–10^7 M} [22–25]. The observed binding constants are more in keeping with the groove binding with DNA, as observed in the literature [26].

Based on the above results, the affinity for DNA is stronger for Yb(III) complex than ligand. We attribute the possible reason is the charge transfer of coordinated H_2L caused by coordination of the central atom results in the decrease of charge density of the planar conjugated system. This change will lead to complexes binding to DNA more easily [7, 8]. Moreover, the helix structure of the Yb(III) complex is able to provide lots of grooving positions to stack more strongly with the base pairs of the DNA helix [27].

In order to further study the binding properties of the compounds with DNA, competitive binding experiment was carried out. Relative binding of H_2L and Yb(III) complex to CT-DNA was studied by the fluorescence spectral method using ethidium bromide (EB)-bound CT-DNA solution in Tris–HCl/NaCl buffer (pH 7.2). As a typical indicator of intercalation, EB is a weakly fluorescent compound. But, in the presence of DNA, emission intensity of EB is greatly enhanced because of its strong intercalation between the adjacent DNA base pairs [7]. In general, measurement of the ability of a complex to affect the intensity of EB fluorescence in the EB–DNA adduct allows determination of the affinity of the complex for DNA, whatever the binding mode may be. If a complex can displace EB from DNA, the fluorescence of the solution will be reduced due to the fact that free EB molecules are readily quenched by the solvent water [28]. For ligand H_2L and the Yb(III) complex, no emission was observed either alone or in the presence of CT-DNA in the buffer. The fluorescence quenching of DNA-bound EB by the ligand and complex are shown in Fig. 6. The behavior of H_2L and Yb(III) complex are in good agreement with the Stern–Volmer equation, which provides further evidence that the two compounds bind to DNA. The K_{sv} values for H_2L and Yb(III) complex are 0.35×10^4 ($R = 0.98$ for 21 points in the line part) and 1.48×10^4 M^{-1} ($R = 0.99$ for 12 points), respectively, reflecting the higher quenching efficiency of the Yb(III) complex relative to that of H_2L. This result suggests that the DNA-binding of the Yb(III) complex is stronger than that of H_2L. Such a trend is consistent with the previous absorption spectral results.

Figure 6 show the plots of I_0/I versus [Component]. The data of K_{sv} are all at 10^4 M^{-1} level for the ligand and the Yb(III) complex, accordingly. In view of the strong interaction of EtBr with DNA of which the binding constant of EtBr with DNA is at 10^6 M^{-1} level [29], we consider it is impossible for the ligand and the complex to scramble EtBr from DNA. A similar fluorescence quenching effect of EtBr bound to DNA has been observed for the addition of several groove-binding compounds, including netropsin and distamycin A [27, 30]. The observed results make us believe that the ligand and the Yb(III) complex may interact with DNA through the groove binding mode, releasing some EtBr molecules from the EtBr–DNA system [30–32].

Antioxidant activities

We compared the abilities of the present compounds to scavenge hydroxyl radicals with those of the well-known natural antioxidants mannitol and vitamin C, using the same method as reported in a previous paper [33]. The 50 % inhibitory concentration (IC_{50}) values of mannitol and vitamin C are about 9.6×10^{-3} and 8.7×10^{-3} M^{-1}, respectively. As shown in Fig. 7a, according to the antioxidant experiments, the IC_{50} value of the Yb(III) complex is 3.35×10^{-5} M^{-1} which implies that the Yb(III) complex exhibits better scavenging activity than mannitol and vitamin C. It can be concluded that much less scavenging activity was exhibited by H_2L when compared to that of the Yb(III) complex which is due to the chelation of the ligand with the central metal atom. Due to the observed IC_{50} values, the Yb(III) complex can be considered as a potential drug to eliminate the hydroxyl radical.

As another assay of antioxidant activity, superoxide radical (O_2^-) scavenging activity has been investigated. The Yb(III) complex has good superoxide radical scavenging activity. The Yb(III) complex shows an IC_{50} value of 4.57×10^{-5} M^{-1} (Fig. 7b), which indicates that it has potent scavenging activity for the superoxide

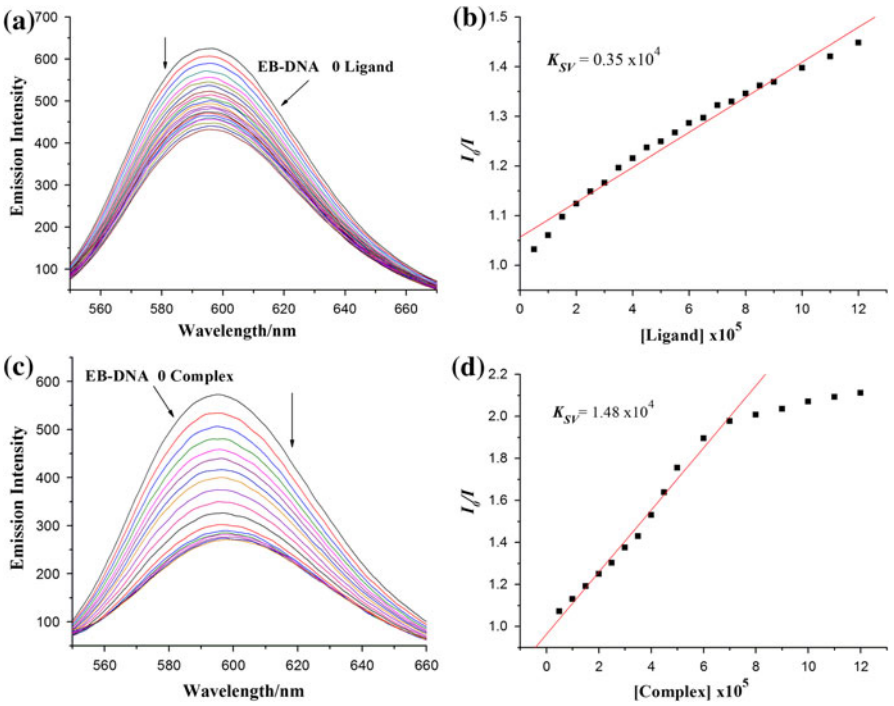

Fig. 6 Emission spectra of EB bound to CT-DNA in the presence of **a** H_2L and **c** Yb(III) complex; [Compound] = 3.0×10^{-5} M; λ_{ex} = 520 nm. The *arrows* show the intensity changes upon increasing concentrations of the complexes. Fluorescence quenching curves of EB bound to CT-DNA by **b** H_2L and **d** Yb(III) complex. (Plots of I_0/I versus [Complex])

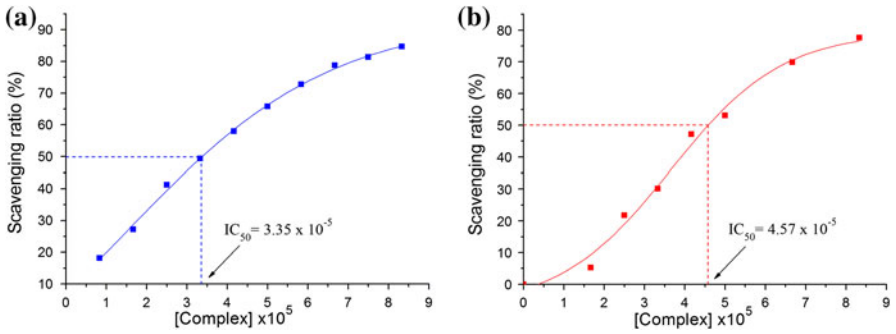

Fig. 7 Plots of antioxidation properties for the Yb(III) complex. **a** The hydroxyl radical scavenging effect (%) for the Yb(III) complex. **b** The superoxideradical scavenging effect (%) for the Yb(III) complex

radical (O_2^-). This indicates that the Yb(III) complex exhibits good superoxide radical scavenging activity and may be an inhibitor (or a drug) to scavenge superoxide radicals (O_2^-) in vivo, an action which needs further investigation.

Conclusions

In this paper, a pentadentate schiff base ligand bis(*N*-salicylidene)-3-oxapentane-1,5-diamine and its Yb(III) complex were synthesized and characterized. The crystal structure of the Yb(III) complex was determined by X-ray crystallography. The binding modes of these compounds with CT-DNA have been studied by electronic absorption titration, EB-DNA displacement experiments, and viscosity measurements. The results indicate that the Yb(III) complex shows higher affinities than the free ligand and interacts with CT-DNA through the groove mode. In addition, the Yb(III) complex also has active scavenging effects on OH and O_2^- radicals. These findings indicate that the Yb(III) complex has many potential practical applications for the development of nucleic acid molecular probes and new therapeutic reagents for diseases on the molecular level. However, its pharmacodynamical, pharmacological, and toxicological properties should be further studied in vivo.

Acknowledgments The present research was supported by the National Natural Science Foundation of China (Grant No. 21367017), the Fundamental Research Funds for the Gansu Province Universities (212086), National Natural Science Foundation of Gansu Province (Grant no. 1212RJZA037), and 'Qing Lan' Talent Engineering Funds for Lanzhou Jiaotong University.

References

1. S. Sreelatha, P.R. Padma, M. Umadevi, Food Chem. Toxicol. **47**, 702–708 (2009)
2. D. Gholamreza, E.N.D. Jafar, J. Abolghasem, A.Z. Karim, M.A. Seyed, K. Soheila, DNA Cell Biol. **30**, 195–201 (2011)

3. C. Hemmert, M. Pitie, M. Renz, H. Gornitzka, S. Soulet, B. Meunier, J. Biol. Inorg. Chem. **6**, 14–22 (2001)
4. G. Zuber, J.C. Quada, S.M. Hecht, J. Am. Chem. Soc. **120**, 9368–9369 (1998)
5. S. Niroomand, M. Khorasani-Motlagh, M. Noroozifar, A. Moodi, J. Photoch. Photobio. B **117**, 132–139 (2012)
6. M.J. Hannon, Chem. Soc. Rev. **36**, 280–295 (2007)
7. H.L. Wu, K.T. Wang, B. Liu, F. Kou, F. Jia, J.K. Yuan, Y. Bai, Inorg. Chim. Acta **384**, 302–308 (2012)
8. H.L. Wu, J.K. Yuan, Y. Bai, G.L. Pan, H. Wang, X.B. Shu, J. Photoch. Photobio. B **107**, 65–72 (2012)
9. H.L. Wu, J.K. Yuan, Y. Bai, G.L. Pan, H. Wang, J. Kong, X.Y. Fan, H.M. Liu, Dalton Trans. **2012**, 8829–8838 (2012)
10. F.H. Lia, G.H. Zhao, H.X. Wu, H. Lin, X.X. Wu, S.R. Zhu, H.K. Lin, J. Inorg. Biochem. **100**, 36–43 (2006)
11. B.D. Wang, Z.Y. Yang, T.R. Li, Bioorgan. Med. Chem. **14**, 6012–6021 (2006)
12. M. Marinić, I. Piantanida, G. Rusak, M. Žinić, J. Inorg. Biochem. **100**, 288–298 (2006)
13. M. Tümer, H. Köksal, M.K. Sener, S. Serin, Trans. Met. Chem. **24**, 414–420 (1999)
14. M.J. Manos, M.S. Markoulides, C.D. Malliakas, G.S. Papaefstathiou, N. Chronakis, M.G. Kanatzidis, P.N. Trikalitis, A.J. Tasiopoulos, Inorg. Chem. **50**, 11297–11299 (2011)
15. W.K. Dong, G. Wang, S.S. Gong, J.F. Tong, Y.X. Sun, X.H. Gao, Trans. Met. Chem. **37**, 271–277 (2012)
16. K. Nakamoto, *Infrared and Raman Spectra of Inorganic and Coordination Compounds*, 4th edn. (Wiley, New York, 1986)
17. L. Casella, M. Gullotti, A. Pintar, L. Messori, A. Rockenbauer, M. Györ, Inorg. Chem. **26**, 1031–1038 (1987)
18. D.S. Sigman, A. Mazumder, D.M. Perrin, Chem. Rev. **93**, 2295–2316 (1993)
19. R. Palchaudhuri, P.J. Hergenrother, Curr. Opin. Biotechnol. **18**, 497–503 (2007)
20. B.D. Wang, Z.Y. Yang, P. Crewdson, D.Q. Wang, J. Inorg. Biochem. **101**, 1492–1504 (2007)
21. H.G. Li, Z.Y. Yang, B.D. Wang, J.C. Wu, J. Organomet. Chem. **695**, 415–422 (2010)
22. V.G. Vaidyanathan, B.U. Nair, J. Inorg. Biochem. **94**, 121–126 (2003)
23. R. Vijayalakshmi, M. Kanthimathi, V. Subramanian, B.U. Nair, Biochim. Biophys. Acta **1475**, 157–162 (2000)
24. H.A. Hussain, K. Iftikhar, Spectrochim. Acta A **59**, 1061–1074 (2003)
25. S. Kashanian, M.B. Gholivand, F. Ahmadia, A. Taravati, A. Hosseinzadeh Colagar, Spectrochim. Acta A **67**, 472–478 (2007)
26. F. Chen, Z. Xu, P. Xi, X. Liu, Z. Zeng, Anal. Sci. **25**, 359–363 (2009)
27. Z.Y. Yang, B.D. Wang, Y.H. Li, J. Organomet. Chem. **691**, 4159–4166 (2006)
28. J.B. LePecq, C. Paoletti, J. Mol. Biol. **27**, 87–106 (1967)
29. M.J. Waring, J. Mol. Biol. **13**, 269–282 (1965)
30. S.M. Nelson, L.R. Ferguson, W.A. Denny, Mutat. Res. **623**, 24–40 (2007)
31. D.L. Boger, B.E. Fink, S.R. Brunette, W.C. Tse, M.P. Hedrick, J. Am. Chem. Soc. **123**, 5878–5891 (2001)
32. Z.Q. Liu, M. Jiang, Y.T. Li, Z.Y. Wu, J.X. Yang, Inorg. Chim. Acta **362**, 1253–1259 (2009)
33. T.R. Li, Z.Y. Yang, B.D. Wang, D.D. Qin, Eur. J. Med. Chem. **43**, 1688–1695 (2008)
34. S. Satyanaryana, J.C. Dabrowiak, J.B. Chaires, Biochemistry **32**, 2573–2584 (1993)
35. J. Marmur, J. Mol. Biol. **3**, 208–218 (1961)
36. S.M. Nalson, V. Knox, J. Chem. Soc. Dalton Trans. **1983**, 2525–2528 (1983)
37. Bruker, *Smart saint and sadabs* (Bruker Axs, Madison, 2000)
38. G.M. Sheldrick, *SHELXTL* (Siemens Analytical X-ray Instruments, Madison, 1996)
39. A.M. Pyle, J.P. Rehmann, R. Meshoyrer, C.V. Kumar, N.J. Turro, J.K. Barton, J. Am. Chem. Soc. **111**, 3051–3058 (1989)
40. A. Wolf, G.H. Shimer, T. Meehan, Biochemistry **26**, 6392–6396 (1987)
41. C.C. Winterbourn, Biochem. J. **198**, 125–131 (1981)
42. Z.Y. Guo, R.E. Xing, S. Liu, H.H. Yu, P.B. Wang, C.P. Li, P.C. Li, Bioorg. Med. Chem. Lett. **15**, 4600–4603 (2005)
43. C. Beauchamp, I. Fridovich, Anal. Biochem. **44**, 276–287 (1971)
44. Q.H. Luo, Q. Lu, A.B. Dai, L.G. Huang, J. Inorg. Biochem. **51**, 655–662 (1993)